Dynamic Characteristics of Transverse Fuel Injection and Combustion Flow-Field inside a Scramjet Engine Combustor

J.-Y. Choi
Department of Aerospace Engineering
Pusan National University, Pusan, 609-735, Korea
aerochoi@pusan.ac.kr

V. Yang and F. Ma
Department of Mechanical Engineering
The Pennsylvania State University, University Park, PA 16802

Keywords: Supersonic Combustion, Combustion Instability, Air-breathing Propulsion, Scramjet Engine, Computational Fluid Dynamics

Abstract

A comprehensive numerical analysis has been carried out for both non-reacting and reacting flows in a scramjet engine combustor with and without a cavity. The theoretical formulation treats the complete conservation equations of chemically reacting flows with finite-rate chemistry of hydrogen-air. Turbulence closure is achieved by means of a k-ω two-equation model. The governing equations are discretized using a MUSCL-type TVD scheme, and temporally integrated by a second-order accurate implicit scheme. Transverse injection of hydrogen is considered over a broad range of injection pressure. The corresponding equivalence ratio of the overall fuel/air mixture ranges from 0.167 to 0.50. The work features detailed resolution of the flow and flame dynamics in the combustor, which was not typically available in most of the previous studies. In particular, the oscillatory flow characteristics are captured at a scale sufficient to identify the underlying physical mechanisms. Much of the flow unsteadiness is related not only to the cavity, but also to the intrinsic unsteadiness in the flow-field. The interactions between the unsteady flow and flame evolution may cause a large excursion of flow oscillation. The roles of the cavity, injection pressure, and heat release in determining the flow dynamics are examined systematically.

Introduction

The success of future high-speed air transportation will be strongly dependent the development of hypersonic air-breathing propulsion engines. Although there exist many fundamental issues, combustor represents one of the core technologies that dictate the development of hypersonic propulsion systems. At a hypersonic flight speed, the flow entering the combustor should be maintained supersonic to avoid the excessive heating and dissociation of air. Thus the residence time of the air in a hypersonic engine is on the order of 1 ms for typical flight conditions. The fuel must be injected, mixed with air and burned completely within such a short time span.

A number of studies have been carried out worldwide and various concepts have been suggested forscramjet combustor configurations to overcome the limitations given by the short flow residence time. Among the various injection schemes, transverse fuel injection into a channel type combustor appears the simplest and has been used in several engine programs, such as the Hyshot scramjet engine, an international program leaded by the University of Queensland.[1] For the enhancement of fuel/air mixing and flame-holding, a cavity is often employed in various supersonic combustion experiments. CIAM of Russia introduced cavities into their engines [2] and U.S. Air Force also employed cavities in the supersonic combustion experiments [3].

From the aspect of fluid dynamics, transverse injection of fluid into a supersonic cross flow and flow unsteadiness associated with a cavity are interesting topics due to their broad applications in many engineering devices. Thus a number of studies have been carried out, and many of them have great relevance to scramjet engines, but a comprehensive study directly applied to combustor dynamics is rarely found. The obstacles lie in the difficulties in conducting high-fidelity experiments and numerical simulations to observe the dynamical phenomena at time and length scales sufficient to resolve the underlying mechanisms. The present study attempts to achieve improved understanding of the unsteady flow and flame dynamics in a realistic scramjet combustor configuration employing a transverse fuel injection and a flame holding cavity. Little is known for this issue from the previous studies.

Theoretical Formulations and Computational Algorithms

Conservation Equations

The combustor configuration is assumed to be two-dimensional for computational efficiency. The conservation equations for a multi-component system are employed to analyze the chemically reacting flow

in a scramjet combustor. The coupled form of the species conservation equations, fluid dynamics equations, and turbulent transport equations can be summarized in a conservative vector form as follows.

$$\frac{\partial \mathbf{Q}}{\partial t}+\frac{\partial \mathbf{F}}{\partial x}+\frac{\partial \mathbf{G}}{\partial y}=\frac{\partial \mathbf{F}_v}{\partial x}+\frac{\partial \mathbf{G}_v}{\partial y}+\mathbf{W} \qquad (1)$$

where the conservative variable vector, **Q**, convective flux vectors, **F** and **G**, diffusion flux vectors, $\mathbf{F}_v$ and $\mathbf{G}_v$, and reaction source term **W** are defined in Eq. (2). Details of the governing equations and thermal properties are described in the literature [4].

$$\mathbf{Q}=\begin{bmatrix}\rho_i\\ \rho u\\ \rho v\\ e\\ \rho k\\ \rho\omega\end{bmatrix},\quad \mathbf{F}=\begin{bmatrix}\rho_i u\\ \rho u^2+p\\ \rho uv\\ (e+p)u\\ \rho ku\\ \rho\omega u\end{bmatrix},\quad \mathbf{G}=\begin{bmatrix}\rho_i v\\ \rho uv\\ \rho v^2+p\\ (e+p)v\\ \rho kv\\ \rho\omega v\end{bmatrix} \qquad (2a)$$

$$\mathbf{F}_v=\begin{bmatrix}-\rho_i u_i^d\\ \tau_{xx}\\ \tau_{xy}\\ \beta_x\\ \mu_k\,\partial k/\partial x\\ \mu_\omega\,\partial\omega/\partial x\end{bmatrix},\quad \mathbf{G}_v=\begin{bmatrix}-\rho_k v_k^d\\ \tau_{xy}\\ \tau_{yy}\\ \beta_y\\ \mu_k\,\partial k/\partial y\\ \mu_\omega\,\partial\omega/\partial y\end{bmatrix},\quad \mathbf{W}=\begin{bmatrix}w_i\\ 0\\ 0\\ 0\\ S_1\\ S_2\end{bmatrix} \qquad (2b)$$

where, $i=1\sim N$.

Combustion Mechanism and Turbulence Closure

The present analysis employs the GRI-Mech 3.0 chemical kinetics mechanism for hydrogen-air combustion [5]. The mechanism consists of eight reactive species (H, H_2, O, O_2, H_2O, OH, H_2O_2 and HO_2) and twenty-five reaction steps. Nitrogen is assumed as an inert gas because the oxidation process does not have significant effect on the fluid dynamics in a combustor. Turbulence closure is achieved by means of Mentor's SST (Shear Stress Transport) model which is based on the k-ω two-equation formulation [6]. This model is the blending of the standard k-ε model that is suitable for a shear layer problem and the Wilcox k-ω model that is suitable for wall turbulence effect[7]. Baridna et al. reported that the SST model shows good prediction for mixing layer and jet flow problems, and that it is also less sensitive to initial values [8].

Another important issue is the closure problems for the interaction of turbulence and chemistry in supersonic conditions. Recently, there were many attempts to address this issue using LES methods, PDF approaches, and other combustion models extended from subsonic combustion conditions. Although much useful advances were achieved, the improvement was significant in comparison with the results from laminar chemistry and existing experimental data, as evidenced in the results by Möbus et al [9]. By examining the existing results, such as Norris and Edwards [10], it is thought that the solution accuracy seems to be more dependent on grid resolution than the modeling of turbulence-chemistry interaction. In view of the lack of reliable models for turbulence-chemistry interactions, especially for supersonic flows, the effect of turbulence on chemical reaction rate is ignored in the present work.

Combustion Mechanism and Turbulence Closure

The governing equations were discretized numerically by a finite volume approach. The convective fluxes were formulated using Roe's FDS method derived for multi-species reactive flows along with the MUSCL approach along with a differentiable limiter function. The spatial discretization strategy satisfies TVD conditions and shows high-resolution shock capturing capability. The discretized equations were temporally integrated using a second-order accurate fully implicit method. A Newton sub-iteration method was also used to preserve the time accuracy and solution stability. Since detailed descriptions of the governing equations and numerical formulation are documented in the previous literature [11], it will not be recapitulated here. The numerical methods has been validated against a number of steady and unsteady simulations of shock-induced combustion phenomena that showed good agreement with existing experimental data [12-13].

Configuration of Scramjet Combustor

Combustor Configuration

The supersonic combustor considered in this study is shown in Fig. 1. The channel type combustor of 10 cm height and 131 cm length is composed of transverse fuel injection and a cavity. This combustor configuration is quite similar to the Hyshot test model, except for the cavity, in which a swallowing slot is employed to remove the boundary layer from the inlet and the combustor starts with a sharp nose [1]. A cavity of 20 cm length and 5cm depth, having an aspect ratio, L/D of 4.0, is employed at 20 cm downstream of the injector.

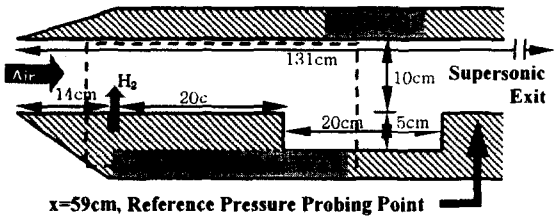

Fig. 1 Frontal part of the scramjet combustor

Operating Conditions

The incoming air flow to the combustor is set to Mach number 3 at 600 K and 1.0 MPa. This combustor inlet condition roughly corresponds to a flight Mach number 5-6 at an altitude of 20 km, although the exact condition depends on the inlet configuration. Gaseous hydrogen is injected vertically through a slot of 0.1 cm width to the combustor through a choked

nozzle. The fuel temperature is set to 151 K. The injector exit pressures are 0.5, 1.0 and 1.5 Mpa, and the overall equivalence ratis are 0.167, 0.33 and 0.5.

Combustor Conditions

A total of 936×160 grids are used for the main-combustor flow passage, and 159×161 grids for the cavity. The grids are clustered around the injector and the solid surfaces and the injector. 54 grid points are included in the injector slot and the minimum grid size near the wall is 70 μm. All the solid surfaces are assumed to be no-slip and adiabatic, except for the upper boundary. For convenience and reduction of the number of grid points required to resolve the boundary layer, the upper boundary is assumed to be a slip wall, which is equivalent to the flow symmetric condition in the present configuration. Extrapolation is used for the exit boundary. Time step is set to 6 ns according to the minimum grid size and the CFL number of 2.0. Four sub-iterations are used at each time step. Figure 2 is a magnified plot of the computational grid around the injector and the fore part of the cavity shown as a dashed-box in Fig. 1.

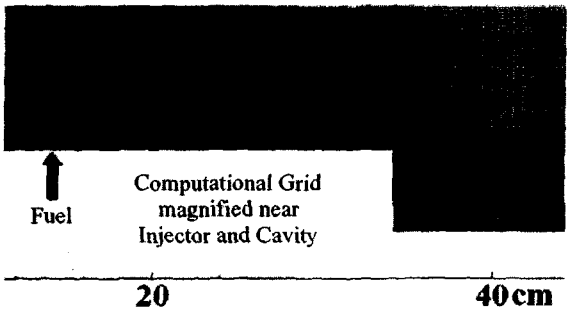

Fig. 2 Magnified plot of computational grid around the injector and the fore part of the cavity.

Results and Discussion

Numerical simulations were carried out for twelve cases, including non-reacting and reacting flows, with andwithout cavity for three different injection pressures of 0.5 1.0 and 1.5 MPa. The following sections will discuss the results for each case. All the cases were run for 6 ms starting from the initial condition, which is longer than the typical test time of the ground based experiments. The plots of the instantaneous flowfields shown in the followings were taken at 5 ms.

Non-reacting Flows Without Cavity

Instantaneous temperature fields for the cases of non-reacting flows without a cavity are plotted in Fig. 3. For the injection pressure ratio of 5.0, the flow field around the injector seems to be quite stable, but a flow disturbance is observed at the location around 40 cm where the first reflected shock wave interacts with the shear layer between the fuel and air flows. The disturbance propagates upstream through the shear layer, but can not reach the injector. Thus the injector flow remains stable and the fuel flow is located very close to the lower surface. The mechanism of the shear layer instability, which is triggered by the impinging oblique shock wave, seems to be the one studied by Papamoschou and Roshko[14].

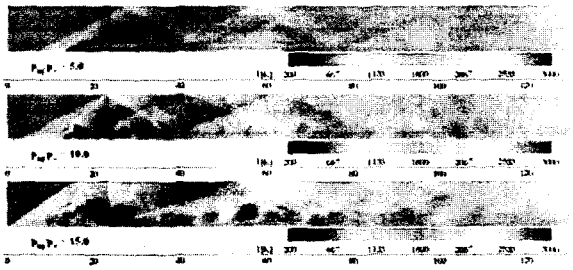

Fig. 3 Instantaneous temperature fields at 5 ms for the case of non-reacting flows without cavity.

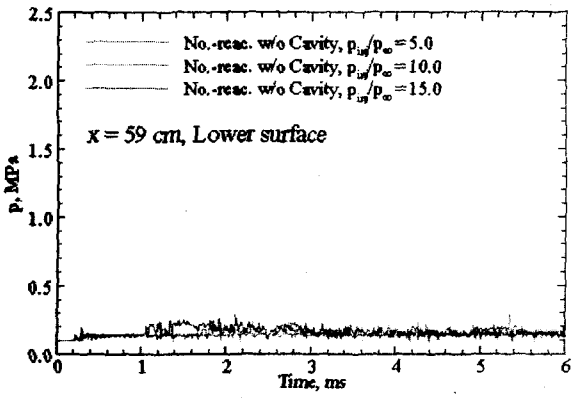

Fig. 4 Time history of pressure for the case of non-reacting flows without cavity.

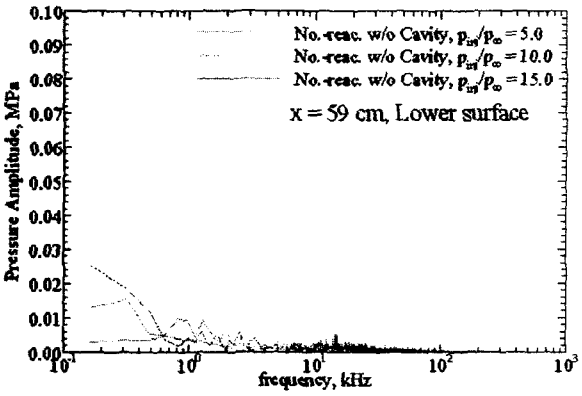

Fig. 5 Frequency spectrum of pressure for the case of non-reacting flows without cavity.

For the injection pressure ratio of 10.0, disturbance was generated during the early stage of the computation in a manner similar to the case of the injection pressure ratio of 5.0. However the disturbance propagates upstream and triggers the injector flow to become unstable. As a result of this interaction, a large portion of the flow area becomes subsonic and the injector flow oscillates strongly. This unstable motion leads to a higher fuel

penetration and the fuel/air mixing is strongly enhanced. This injector flow instability mechanism has been observed by Papamoschou and Hubbard [15]. Ben-Yakar et al. also observed essentially the same unstable injection jet in their supersonic combustion experiment [16]. For the injection pressure ratio of 15.0, the injector flow instability is getting stronger and oscillatory flows are observed in the entire combustor field. Thus the fuel penetrates around the middle of the combustor and the fuel/air mixing is greatly enhanced.

Figure 4 shows the temporal variation of the pressure at the location, of x=59 cm from the leading edge of the lower surface. This location is 5 cm downstream of the end of cavity, and is selected because it may reflect all the upstream influences from the injector and cavity. The pressure variations in Fig. 4 reflect the instability characteristics discussed above. The curve for the injection pressure ratio of 5.0 shows oscillations generated from the disturbances in the shock wave/shear layer interaction region, but remains nearly stable maintaining the pressure about 0.15MPa. Similar results are obtained for the pressure ratios of 10.0 and 15.0. However, the flowfield becomes strongly unstable at 1.8 ms for the pressure ratios of 10.0 and at 1.0 ms for the pressure ratio of 15.0. These instances are the time when the injector flows become unstable. After some transitional period between 1 to 2 ms, steady oscillations are reached.

Figure 5 shows the frequency spectrum of the pressure oscillation obtained from an FFT (Fast Fourier Transformation) analysis. Since the total computing time is 6 ms, the low frequency portion in the plot is not the dominant instability frequencies. The dominant frequency that can be observed is located in the frequency around 15 kHz observed for the pressure ratios 10.0 and 15.0.

Non-reacting Flows With Cavity

Figure 6 shows the instantaneous temperature fields for the case of non-reacting flows with a cavity. The cavity plays an important role in disturbing the flow field and mixing the fuel and air. What is different from the cases without cavity is that the cavity generates disturbances which in turn trigger the injector flow to become unstable even for the case with a low injection pressure ratio of 5.0. Thus, the injector flow becomes unstable for all the pressure ratios under conditions with a cavity. The fuel penetration and fuel/air mixing seems to be enhanced by the oscillating mechanism of the cavity.

Figure 7 shows the plots of the pressure variation at the location of x=59 cm. For all the three injection pressure ratios, the injector instability is triggered by the cavity induced instability within 1 ms, which is around the half of the value for the cases without a cavity. Also the pressure fluctuation is much stronger and the pressure level is maintained slightly higher than the cases without a cavity.

Figure 8 shows the frequency spectrum for this case. Unlike the above case, the dominant frequency is not at 15 kHz, but around 1.5~2.5 kHz and 4~6 kHz. although there are some dependency on the injection pressure ratio. The expected cavity oscillation frequencies from Rossiter's semi empirical formula discussed by Ben-Yakar and Hanson [17] are 1.9 kHz for the first mode and 4.5 kHz for the second mode for the flow conditions in this study. Thus the present computational simulations give quite satisfactory results, considering the complex flow structures involving shock waves and fuel injection.

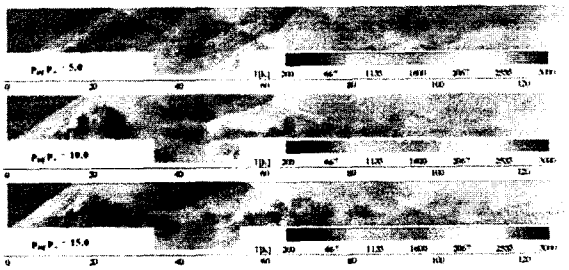

Fig. 6 Instantaneous temperature fields at 5 ms for the case of non-reacting flows with cavity.

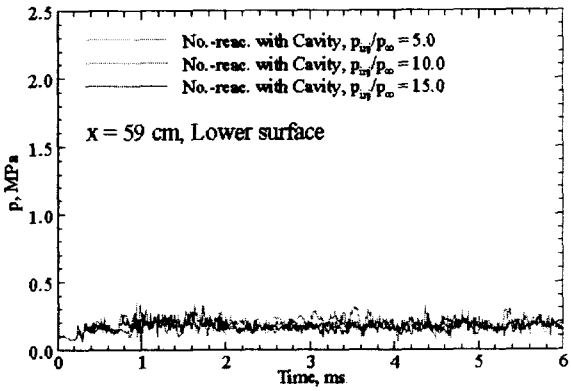

Fig. 7 Temporal variation of pressure for the case of non-reacting flows with cavity.

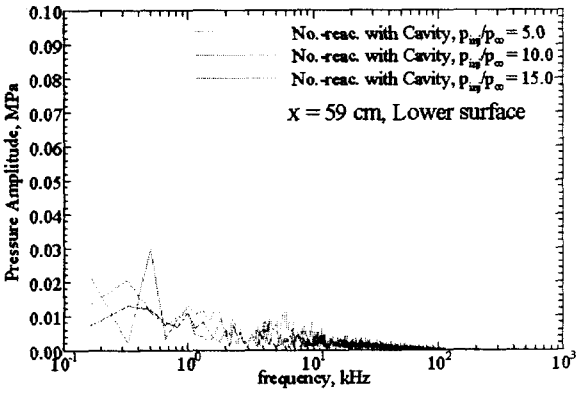

Fig. 8 Frequency spectrum of pressure for the case of non-reacting flows with cavity.

Reacting Flows Without Cavity

Figure 9 shows the instantaneous temperature fields for reacting flows without a cavity. For the injection

pressure ratio of 5.0, combustion occurs in the frontal separation region, but is not fully established along the shear layer. This separation region contains a pool of radicals and acts as a preheating zone. The flame is not anchored there, but in the region containing shock-wave/shear-layer interaction where the instability is generated. Downstream of this location, heat release from chemical reactions takes place, accompanied with large vortices convecting downstream. The overall phenomena seem quite similar to a typical turbulent diffusion flame generating large vorticities. It is thought from this result that chemical reactions do not intensify the disturbance to an extent sufficient for triggering the instability of the injector flow.

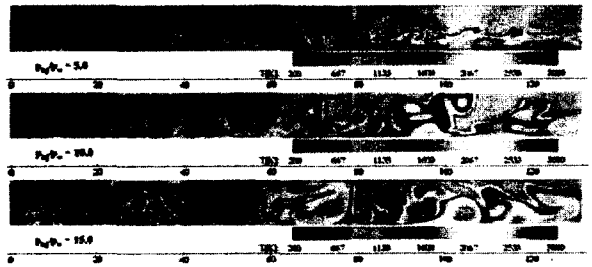

Fig. 9 Instantaneous temperature fields at 5 ms for the case of reacting flows without a cavity.

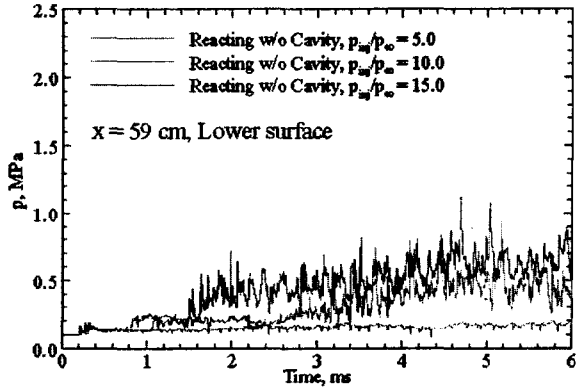

Fig. 10 Pressure-time history for the case of reacting flows without a cavity.

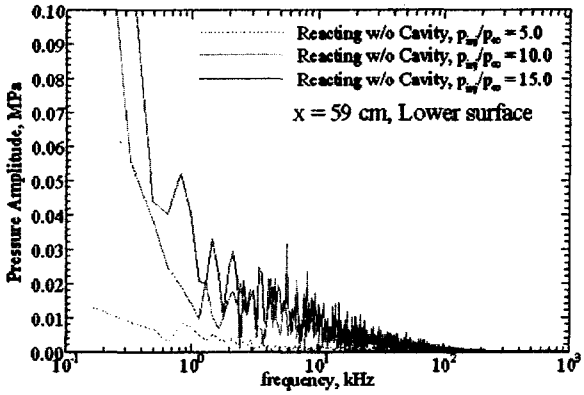

Fig. 11 Frequency spectrum of pressure for the case of reacting flows without a cavity.

For the injection pressure ratios 10.0 and 15.0, the temperature fields show different characteristics. Due to the large heat release, the pressure behind the injector builds up and leads to a Mach reflection across the combustor. A large subsonic region is formed downstream of the injector, and the injector flow no longer shows a structure composed of a leading oblique shock wave, a frontal separation region, etc. Instead, the fuel is injected though a narrow with of subsonic jet, but can penetrate much deeper. The frontal separated flow region, which has a role as a radical pool and a pre-heater, still exists for the injection pressure ratio of 10.0, but disappears for the injection pressure ratio of 15.0 due to the fully subsonic environment near the injector. The frontal separated flow region and the oblique shock wave extends to the leading edge of the combustor and is stabilized there by the fixed inlet boundary condition.

Figure 10 shows the temporal evolution the pressure for the reacting flows without a cavity. For the injection pressure ratio of 5.0, the final pressure is slightly higher than that of the non-reacting case and the pressure builds up very slowly. In contrast to this case, the results for the pressure ratios of 10.0 and 15.0 indicate that the injector instability is triggered around 1 ms and the pressure build-up is established around 3 ms for the pressure ratio of 10.0 and 1.5 ms for the the ratio of 15.0. The pressure reaches approximately 0.5MPa for the pressure ratio of 10.0 and 0.6 MPa for the pressure ratio of 15.0. The flowfields for both cases are nearly stabilized around this condition.

Figure 11 shows the frequency spectrum for this case. Unlike the non-reacting cases, a dominant frequency is not observed for all the cases and the spectra are widely distributed, although the low frequency range less than 10 kHz dominates the overall spectrum.

Reacting Flows With Cavity

Figure 12 shows the instantaneous temperature fields for the reacting flows with a cavity. For the injection pressure ratio of 5.0, combustion is fully established over the cavity, and the cavity acts as a flame holder or a radical pool. The pressure builds up to around 0.3MPa, which is much greater than the case without a cavity. For the injection pressure ratios of 10.0 and 15.0, the pressure builds up rapidly and the combustor seems to be choked. The Mach reflection continuously develops and is finally disgorged out of the inlet. The pressure-time history shown in Fig. 13 indicated that the combustion is established much earlier than the cases without a cavity for all the injection pressure ratios. This is caused by the mixing and combustion enhancement by the cavity that can be understood by comparing the pressure variations in Figs. 7 and 10. The frequency spectrum in Fig. 14 does not exhibit any major frequency but the dominancy is less than 10kHz as was the reacting flows without a cavity.

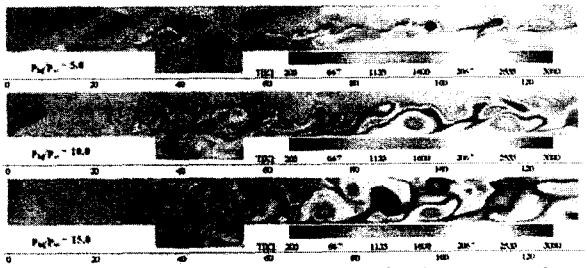

Fig. 12 Instantaneous temperature fields at 5 ms for the case of reacting flows without a cavity.

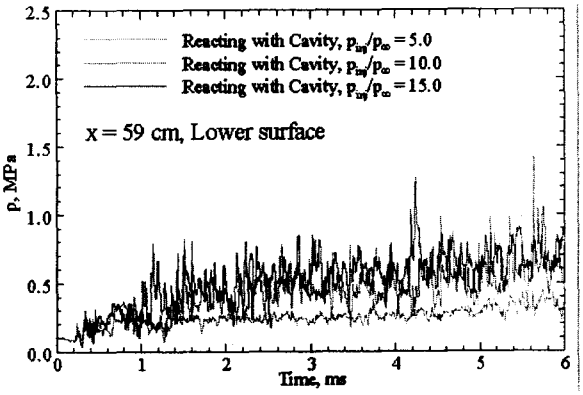

Fig. 13 Pressure-time history for the case of reacting flows with a cavity.

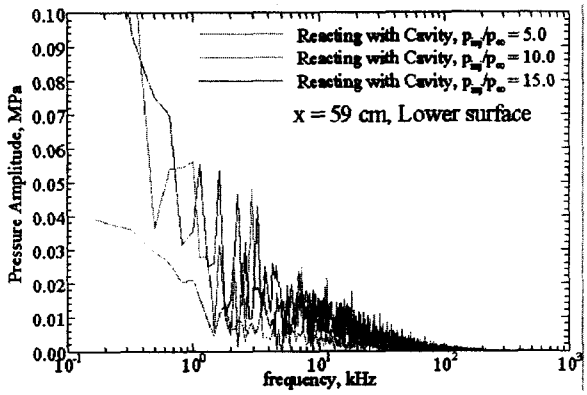

Fig. 14 Frequency spectrum of pressure for the case of reacting flows with a cavity.

Conclusion

The reacting flow dynamics in a scramjet combustor was carefully studied by means of a comprehensive numerical analysis. The present results show a wide range of phenomena resulting from the interactions among the injector flows, shock waves, shear layers, and oscillating cavity flows. As a conclusion of the present study, new findings can be summarized as follows.

1) Strong unsteady flow characteristics were identified for a scramjet combustor. The work appears to be the first of its kind in the numerical study of combustion oscillations in a supersonic combustor.

2) Large flow disturbances can be generated by shear layer instability that may be triggered by the interactions with shock waves.

3) For all the cases studied herein, instability caused by the cavity seems to override the shear layer instability caused by the shock-wave/shear-layer interactions when both instabilities are present.

4) Transverse injected jet may remain stable without disturbance, but can be triggered to become unstable with disturbances from a shear layer or a cavity. Disturbed transverse injected jet has deeper penetration and improved fuel/air mixing than the stabilized one. A more careful study is necessary to characterize the stability of transverse injection jets.

5) The roles of the cavity as a source of disturbance for the transverse jet, fuel/air mixing enhancement, and flame holder were clarified.

6) Unstable flow characteristics for the reacting cases are similar to that of non-reacting flows except for the cases where pressure builds up rapidly.

7) When the combustion takes place throughout the entire chamber, an unstable Mach reflection is formed above the injector and the pressure builds high enough for propulsion applications.

8) The Mach reflection is unstable due the flow unsteadiness and results in a strong pressure fluctuation on the upper wall.

9) As an extreme case of high pressure build up, thermal choking of the combustor was observed, which resulted in the combustor unstart by the forward running strong shock wave.

10) The present study can be extended to a more realistic combustor configuration, but further investigations are necessary to achieve better understanding of detailed fluid and flame a scramjet combustor.

References

1) Centre for Hypersonics - HyShot Scramjet Test Programme, http://www.mech.uq.edu.au/hyper/hyshot/

2) McClinton, C., Roudakov, A., Semenov, V. and V. Kopehenov, "Comparative flow path analysis and design assessment of an axisymmetric hydrogen fueled scramjet flight test engine at a Mach number of 6.5," AIAA Paper 96-4571, VA, Nov. 1996

3) Mathur, T., Gruber, M. Jackson, K., Donbar, J., Donaldson, W., Jackson, T and Billig, F., "Supersonic Combustion Experiments with a Cavity-Based Fuel Injector, Journal of Propulsion and Power, Vol.17 No.6, 2001, pp.1305-1312.

4) Choi, J. Y., Jeung, I. S. and Yoon, Y., "Numerical Study of SCRam-Accelerator Starting Characteristics," AIAA Journal, Vol. 36, No. 6, 1998, pp. 1029-1038.

5) Smith, G. P., Golden, D. M., Frenklach, M., Moriarty, N. W., Eiteneer, B., Goldenberg, M., Bowman, C.T., Hanson, R.K., Song, S., Gardiner

Jr., W.C., Lissianski, V.V., and Qin, Z., GRI-Mech, http://www.me.berkeley.edu/gri_mech/

6) Menter, F. R., "Two-Equation Eddy-Viscosity Turbulence Models for Engineering Application," AIAA Journal, Vol. 32, No. 8, 1994, pp.1598-1605.
7) Wilcox, D. C., Turbulence Modeling for CFD, DCW Industries, La Cañada, CA, 1993.
8) Bardina, J. E., Huang, P. G., and Coakly, T. J., "Turbulence Modeling Validation," AIAA 97-2121, 1997.
9) Möbus, M., Gerlinger, P. and Brüggermann, "Scalar and Joint scalar-Velocity-Frequency Monte Carlo PDF simulation of Supersonic Combustion," Combustion and Flame, Vol. 132, 2003, pp.3-24.
10) Norris, J. W. and Edwards, J. R., "Large-Eddy Simulation of High-Speed Turbulent Diffusion Flames with Detailed Chemistry," AIAA Paper 97-0370, 1997.
11) Choi, J.-Y., Jeung, I.-S. and Yoon, Y., "Computational Fluid Dynamics Algorithms for Unsteady Shock-Induced Combustion, Part 1: Validation," AIAA Journal, Vol. 38, No. 7, July 2000, pp.1179-1187.
12) Choi, J.-Y., Jeung, I.-S. and Yoon, Y., "Unsteady-State Simulation of Model Ram Accelerator in Expansion Tube," AIAA Journal, Vol. 37, No. 5, 1999, pp.537-543.
13) Choi, J.-Y., Jeung, I.-S. and Yoon, Y., "Scaling Effect of the Combustion Induced by Shock Wave/ Boundary Layer in Premixed Gas," Proceedings of the Combustion Institute, Vol. 27, 1998, pp. 2181-2188.
14) Papamoschou, D., and Roshko, A., "The Turbulent Compressible Shear Layer: An Experimental Study," Journal of Fluid Mechanics, Vol. 197, 1988, pp. 453-477.
15) Papamoschou, D., and Hubbard, D.G., "Visual Observations of Supersonic Transverse Jets," Experiments in Fluids, Vol. 14, May 1993, pp. 468-471., http://supersonic.eng.uci.edu/scramjet.htm
16) Ben-Yakar, A., Kamel, M .R., Morris, C. I. and Hanson, R. K., "Experimental Investigation of H2 Transverse Jet Combustion in Hypervelocity Flows," AIAA Paper 97-3019, 1997.
17) Ben-Yakar, A. and Hanson, R. K., "Cavity Flame-Holders for Ignition and Flame Stabilization in Scramjets: An Overview," Journal of Propulsion and Power, Vol. 17, No. 4, 2001, pp.869-877.